

Dielectrophoretic Batch Fabrication of Bundled Carbon Nanotube Thermal Sensors

Carmen K. M. Fung, *Student Member, IEEE*, Victor T. S. Wong, *Student Member, IEEE*,
Rosa H. M. Chan, *Student Member, IEEE*, and Wen J. Li, *Member, IEEE*

Abstract—We present a feasible technology for batch assembly of carbon nanotube (CNT) devices by utilizing ac electrophoretic technique to manipulate multiwalled bundles on an Si/SiO₂ substrate. Based on this technique, CNTs were successfully and repeatedly manipulated between microfabricated electrodes. By using this parallel assembly process, we have investigated the possibility of batch fabricating functional CNT devices when an ac electrical field is applied to an array of microelectrodes that are electrically connected together. Preliminary experimental results showed that over 70% of CNT functional devices can be assembled successfully using our technique, which is considered to be a good yield for nanodevices manufacturing. Besides, the devices were demonstrated to potentially serve as novel thermal sensors with low power consumption (~microwatts) with electronic circuit response of approximately 100 kHz in constant current mode operation. In this paper, we will present the fabrication process of this feasible batch manufacturable method for functional CNT-based thermal sensors, which will dramatically reduce production costs and production time of nanosensing devices and potentially enable fully automated assembly of CNT-based devices. Experimental results from the thermal sensors fabricated by this batch process will also be discussed.

Index Terms—AC electrophoretic manipulation, carbon nanotube (CNT), CNT sensors, nano batch fabrication, nanomanufacturing.

I. INTRODUCTION

CARBON NANOTUBES (CNTs), since discovered in 1991 by Iijima [1], have been extensively studied for their electrical (e.g., see [2]) and mechanical properties (e.g., see [3]). Owing to their minute dimensions and good mechanical and electrical properties, different groups began to utilize CNTs as nanosensors or actuators for different applications in nanoelectronic or nanoelectromechanical systems (NEMS). For example, the CNT has been found to be an excellent one-dimensional (1-D) quantum wire [2], nanotransistor [4],

molecular random access memory [5] for nanoelectronic applications, and more recently, the nanomotor with a CNT as a rotational shaft for NEMS application [6].

In order to build practical CNT-based devices, fast and batch techniques to manipulate CNTs have to be developed. However, CNTs tend to cling together in nature due to the presence of strong surface charges on their surfaces. The difficulty of isolating a single CNT from an intertwined bundle without tremendous effort in the sense of batch fabrication has led to a clear boundary between the two approaches of the usage of CNTs: either to treat each CNT as an individual building element or to treat CNT bundles (or array) as a whole building block.

To fabricate a nanodevice with CNTs as individual building elements, the basic requirements include the isolation, manipulation, transport, fixture and connection, etc. of a single CNT. A typical manipulation technique is by atomic force microscopy (AFM) [7] and a variety of mechanical and electronic nanodevices have been fabricated by using AFM-based assembly method (e.g., see [8]). However, even though the AFM-based technique has very high positioning accuracy, this pick-and-place technique is time consuming, and few efforts have been reported to tackle the fundamental problem of the inefficiency caused by AFM operations when the process turns into batch production. Among which, Kim *et al.* have reported a method to align CNTs side by side by means of condensation of a nanowire solution [9], [10]. On the other hand, bypassing the complex AFM operations completely, some of the nanodevice researchers have shifted to focus on treating CNT/nanowire bundles as an individual functional (e.g., sensing) element. By means of chemical vapor deposition (CVD), in combination with lithography techniques [11] or laser trimming [12], “vertically” aligned CNT/nanowires can be grown and patterned on specific sites in batch mode. The nanodevices developed based on this approach generally treat a bundle of aligned CNT/nanowires as one functional (i.e., sensing, emitting, etc.) element. By patterning an array of “functional bundle,” a functional array is formed. On the other hand, electric-field assist assembly is another feasible technology in batch fabrication of CNT/nanowires devices. Yamamoto *et al.* have pioneered the work in electric-field assist manipulation of CNT bundles [13], [14]. The usage of electric-field assist assembly has also been reported for batch assembly of nanowires as well [15]. Recently, Nagahara *et al.* have demonstrated the manipulation of CNT strands by ac bias voltage to form functional nanoresistive device between a pair of nanoelectrodes [16]. Based on the technique of electric-field assist assembly (i.e., ac electrophoresis), we have successfully manipulated bundled CNTs to connect between an array of

Manuscript received August 12, 2003; revised April 2, 2004. This work was supported by the Hong Kong Research Grants Council under Grant CUHK4206/00E and Grant 4381/02E, and by the Chinese Academy of Sciences’ Distinguished Overseas Scholar Grant. This paper is based on work presented at the IEEE International Conference on Nanotechnology, San Francisco, CA, August 2003.

C. K. M. Fung and R. H. M. Chan are with the Centre for Micro and Nano Systems, The Chinese University of Hong Kong, Shatin, Hong Kong.

V. T. S. Wong was with the Centre for Micro and Nano Systems, The Chinese University of Hong Kong, Shatin, Hong Kong. He is now with the Department of Mechanical and Aerospace Engineering, University of California at Los Angeles, Los Angeles, CA 90095 USA (e-mail: assayer@ieee.org).

W. J. Li is with the Centre for Micro and Nano Systems, The Chinese University of Hong Kong, Shatin, Hong Kong and also with the Shenyang Institute of Automation, Shenyang 110016, China (e-mail: wen@acaе.cuhk.edu.hk).

Digital Object Identifier 10.1109/TNANO.2004.834156

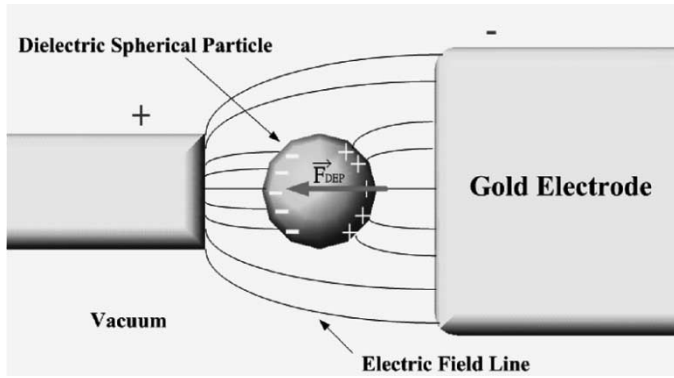


Fig. 1. Dielectric spherical particle undergoing DEP motion. The unbalanced force impart on the sphere is causing it to move toward the smaller electrode. This figure shows the charge distribution in a particular instant where the small electrode is at a higher potential than the large electrode. For ac bias voltage, the potential will be interchanged periodically on the electrodes and the resulting force on the particle is still acting on the same direction due to uneven electric-field distribution.

microelectrodes and we have also preliminarily proven that a CNT device is capable of very low power thermal sensing and can be fabricated in a fast and efficient manner.

This paper reports the ac electrophoretic technique to form bundled MWNT resistive elements between gold (Au) microelectrodes, which were fabricated by a standard microlithographic technique. In addition, the experimental results showing the validity of batch assembling of arrays of CNT sensors by ac bias electrophoresis will be presented. Besides, the electrical performance of the assembled CNT devices such as I - V characteristics, frequency response and temperature coefficient of resistance (TCR) will be characterized and presented in later sections.

II. AC ELECTROPHORETIC MANIPULATION OF CNT

A. Theoretical Background and Modeling

AC electrophoresis (or dielectrophoresis) is a phenomenon where neutral particles undergo mechanical motion inside a nonuniform ac electric field [17] (see Fig. 1).

In our CNTs manipulation experiments, CNTs were dispersed inside a liquid medium (e.g., ethanol) and, therefore, other forces (e.g., viscous force) besides dielectrophoretic (DEP) forces are imparted on CNTs during the manipulation process. In order to understand the physical phenomenon during the ac electrophoretic manipulation, we have conducted the following simulations with experimental verifications on the effect of CNT alignments on different microelectrode geometries.

During the CNTs manipulation, the total force acting on a multi-walled carbon nanotube (MWNT) is the sum of a number of independent forces [18], [19]. With negligible gravitational force, the three dominate force components are the DEP force, viscous force, and the electrothermal force. For other small particles with volumes compatible to an MWNT, thermal effects can dominate, but the high polarizability of an MWNT makes the DEP force large enough to produce deterministic movements.

Dielectrophoresis refers to the force exerted on a polarized particle in the nonuniform electric field [17], [20]. It can be written as

$$\mathbf{F}_{\text{DEP}}(t) = (\mathbf{m}(t) \cdot \nabla) \mathbf{E}(t) \quad (1)$$

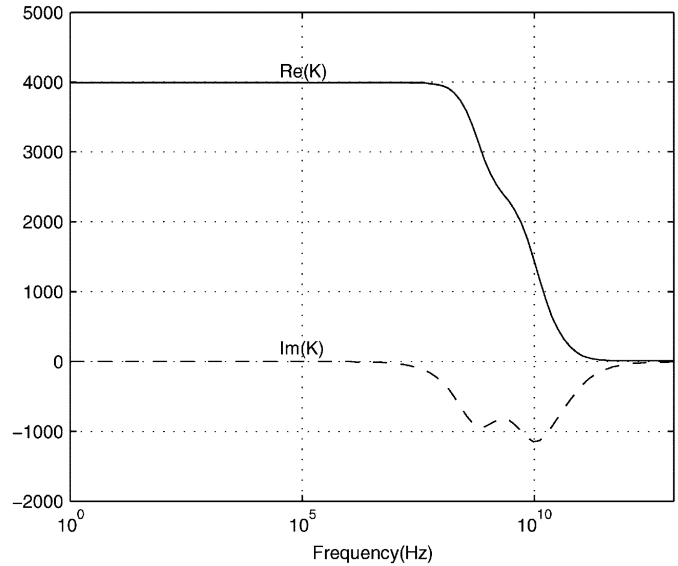


Fig. 2. Complex polarization factor K when the longest axis of the MWNT is parallel to the electric field applied.

where E is the electric field and m is the induced dipole moment of the MWNT. Assuming that the MWNT is a long prolate spheroid with the longest axis aligned with the electric field, the induced dipole moment is

$$\mathbf{m}(t) = 4\pi\epsilon_m ab^2 K \mathbf{E}(t) \quad (2)$$

where ϵ_m , a and b are absolute permittivity of the medium, the half-length of the MWNT, and the radius of the MWNT, respectively. Therefore, the complex polarization factor K is given by

$$K = \frac{\epsilon_p^* - \epsilon_m^*}{3[\epsilon_m^* + (\epsilon_p^* - \epsilon_m^*)L_{||}]} \quad (3)$$

where ϵ_p^* and ϵ_m^* are the absolute complex permittivities of the MWNT [21] and the medium (ethanol) [22], respectively, and the approximated depolarization factor [20] $L_{||} \approx (b^2/a^2)[\ln(2a/b) - 1]$. Since the electric-field components are in-phase, the time-averaged DEP force deduced from the above equations is

$$\langle \mathbf{F}_{\text{DEP}}(t) \rangle = 2\pi ab^2 \epsilon_m \text{Re}(K) \nabla |\mathbf{E}_{\text{rms}}|^2 \quad (4)$$

where $\nabla |\mathbf{E}_{\text{rms}}|^2$ is the gradient of the square of the root mean square (rms) of the electric field. The gradient is affected by both the geometry of the electrodes and the applied voltage. The former factor gives the overall position of the MWNT branches between the electrodes because it determines the direction of the average DEP force. As the potential difference applied is proportional to the magnitude of the electric field, a larger potential can increase the magnitude of the DEP force and offer a larger torque to align the MWNT with the electric-field direction [20].

Frequency of the applied voltage also affects the magnitude of DEP force as the complex permittivity spectra of the MWNT and ethanol are the functions of the frequency [21]–[23]. Due to the high conductivity of the assumed purified MWNT ($\approx 2.22 \times 10^4$ S/m) [21] and the small depolarization factor resulted from its long dipole ($L_{||} \approx 8.3434 \times 10^{-5}$), the real part of the complex polarization factor is positive, as shown in Fig. 2. Although the actual complex polarization factor varies, which is because

the absolute permittivity and the orientation of each MWNT varies [21], $\text{Re}(K)$ remains positive. When substituting different permittivity values at 1 MHz, the DEP force is maximum when the longest axis is parallel to the electric field ($\text{Re}(K) \approx 3995.2$). By substituting L_{\parallel} with $L_{\perp} \approx 0.5$ in (3), the minimum DEP force can be calculated when it is perpendicular to the field ($\text{Re}(K) \approx 0.6667$). The corresponding positive DEP force draws the MWNT to the electric field maxima.

Another factor affecting the magnitude of the force is the volume of the MWNT, as shown in (4). In the MWNT manipulation experiment, the MWNT with axial length and diameter of approximately $1\text{--}10\ \mu\text{m}$ and $10\text{--}30\ \text{nm}$, respectively, was used and, therefore, $a = 2.5\ \mu\text{m}$ and $b = 10\ \text{nm}$ are taken as the averages in the simulation.

A few microelectrodes with different geometries were fabricated and the CNT connections across the microelectrodes by ac electrophoresis are shown in Fig. 3(a)–(c). Detailed experimental procedures in forming CNT bundles across microelectrodes will be presented in Section II-B. However, in order to visualize the electric-field distribution generated by different microelectrode geometries, simulations were conducted and are described in Section II-B.

The approximate order-of-magnitude of the potential was investigated by using Green's theorem [24], where the square of the rms magnitude of the field is calculated using MATLAB. Since the magnitude of the electric field decreases with height away from the substrate, the positive DEP draws the MWNT downwards to the edges of the electrodes. The force fields in Figs. 4 and 5 are estimated by (4), assuming the longest axes of the MWNT is parallel to the instantaneous electric field.

Downward forces are shown by the contours in Fig. 4(a) and (b) between the electrodes and close to the electrode surfaces. The DEP forces are significantly large to draw the MWNT downwards and to overcome the upward movement from the electrothermal effect [19].

The time-averaged alignment torque acting on the MWNT causes them to direct as the electric-field vectors. As the electric-field intensity is higher at the closest corners between electrodes, the MWNTs are drawn to their edge. When an MWNT touches one of the electrodes, it shares the same potential as the electrode and, thus, the electric-field intensity is modified to be higher at its free end. Therefore, the nanotubes near it tend to stick to it. When the nanotube bridges the adjacent voltages, the branching structures between electrodes are formed [13], as shown in Fig. 3. Details of experimental procedures for the ac electrophoretic manipulation of the MWNT will be presented in Section II-B.

B. Experimental Details and Results

Based on the physical phenomenon of ac electrophoresis, we have successfully manipulated the bundled CNTs on fabricated microelectrodes. The experimental process flow for the CNTs manipulation can be divided into three parts, which are: 1) fabrication of microelectrodes; 2) sample preparation; and 3) experimental testing (see Fig. 6).

The Au microelectrodes were fabricated on glass or Si/SiO₂ substrates by a standard microfabrication technique, which was described previously in [25]. Prior to the MWNT manipulation,

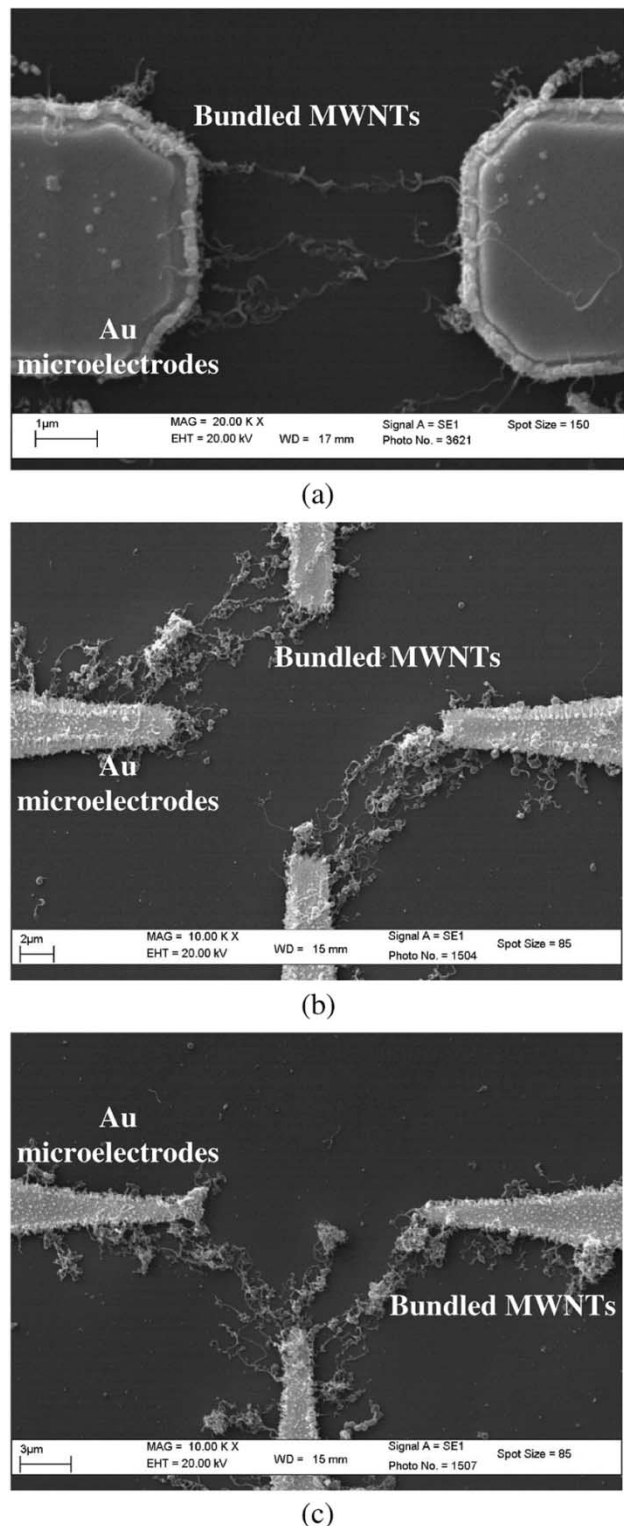


Fig. 3. Experimental alignments of MWNT branches when ac voltage (16 V peak-to-peak at 1 MHz) is applied for: (a) a pair of parallel electrodes, (b) cross electrodes, and (c) T-electrodes.

bundled MWNTs were prepared by a sonication treatment. The bundled MWNTs used in the experiments were ordered commercially from the Sun Nanotech Company Ltd., Beijing, China, which were prepared by CVD. The axial dimension and the diameter of the MWNTs was $1\text{--}10\ \mu\text{m}$ and $10\text{--}30\ \text{nm}$, respectively. In order to minimize the degree of aggregation,

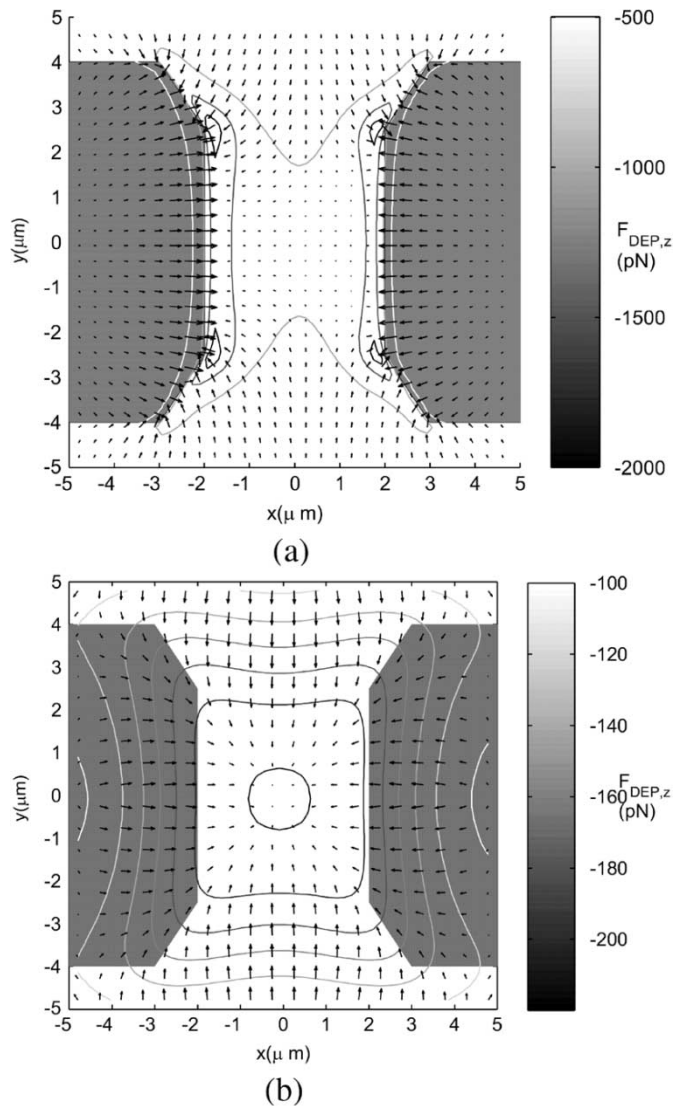


Fig. 4. Average DEP force between the electrodes, which were applied by 16-V peak-to-peak ac voltage at 1 MHz. Arrows are the force vectors on the x - y -plane: (a) at $1 \mu\text{m}$ and (b) $3 \mu\text{m}$, respectively, above the electrodes in Fig. 3(a). The contours represent the order of downward forces.

50 mg of the sample was ultrasonically dispersed in a 500-mL ethanol solution, and the resulting solution was diluted to 0.01 mg/mL for later usage.

During the CNTs manipulation, a substrate with fabricated Au microelectrodes was placed on the vacuum-pump-based stage of a micromanipulator station, which allowed the probing of microelectrodes by microprobes. Au microelectrodes were then excited by an ac voltage source with typically 16-V peak-to-peak with a frequency of 1 MHz. Approximately $10 \mu\text{L}$ of the MWNTs/ethanol solution was transferred to the substrate by a 6-mL gas syringe. The ethanol was evaporated away leaving the MWNTs to reside between the gaps of the microelectrodes. We have observed from the experimental results that bundled MWNTs was attracted toward the Au microelectrodes under nonuniform electric field (see Fig. 7) and connected across the microelectrodes. A representative scanning electron microscopic (SEM) image showing the bridging of MWNTs across the Au microelectrodes is shown in Fig. 8.

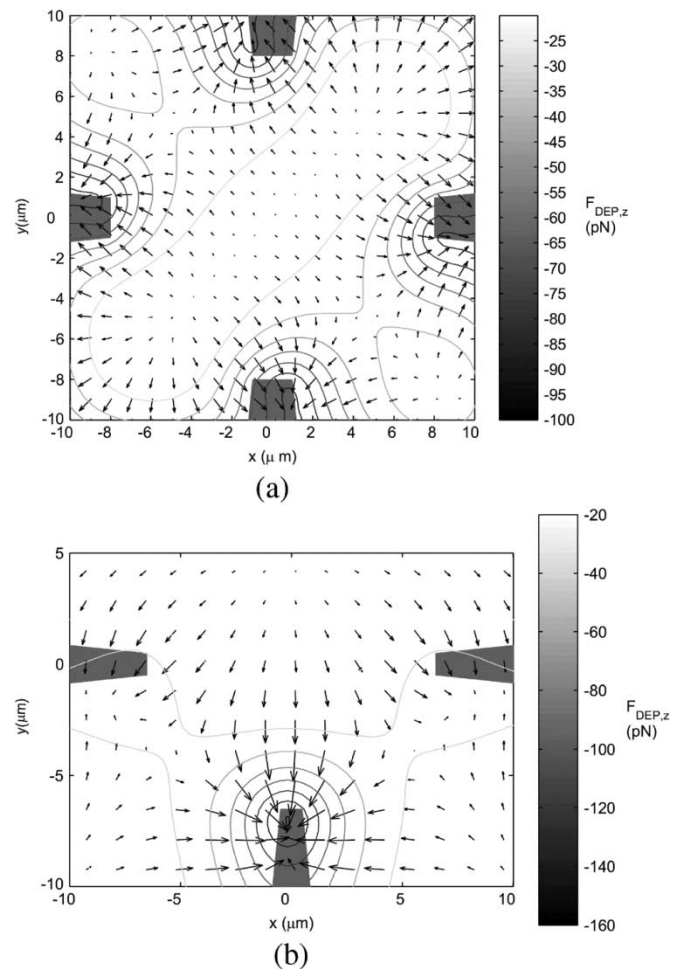
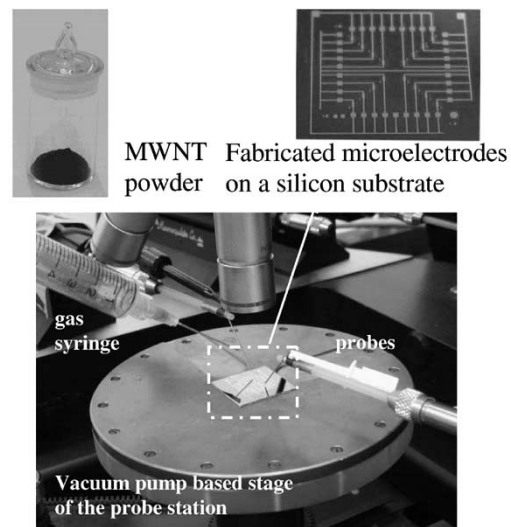


Fig. 5. Average DEP force between the electrodes when ac voltage (16-V peak-to-peak at 1 MHz) is applied for: (a) cross electrodes and (b) T-electrodes at $3 \mu\text{m}$ above the surface.



Excitation of the circuit by AC voltage source and transferring of the MWNT/ethanol suspension to the substrate

Fig. 6. Experimental setup for CNT manipulation by using ac electrophoresis.

The formation of MWNTs linkages can be further confirmed by testing the connectivity between the pair of microelectrodes.

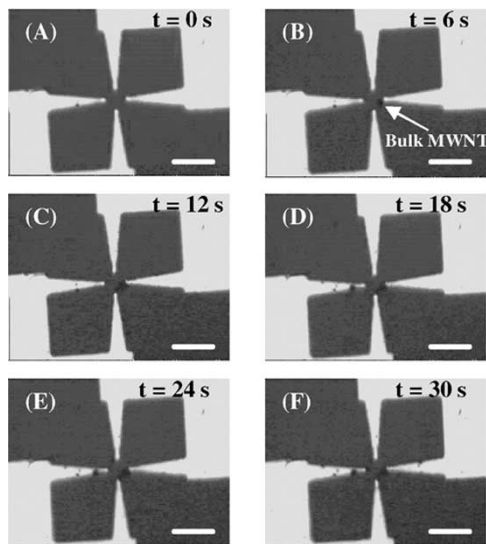


Fig. 7. (A)–(F) Optical microscopic images showing the process of ac electrophoretic manipulation of bulk MWNTs. Consecutive pictures were captured with 6-s intervals. (Scale bar = 20 μm).

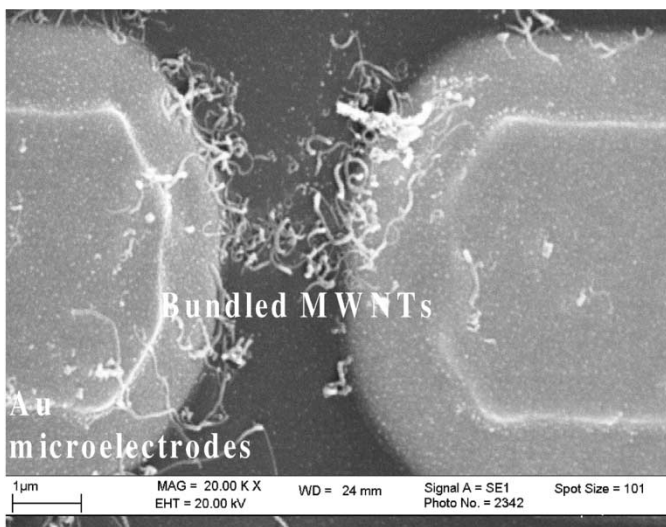


Fig. 8. SEM image showing the formation of MWNTs between a pair of parallel Au microelectrodes.

For instance, room-temperature resistances between the microelectrodes were measured and the two-probe room-temperature resistances of the samples typically range from several to several hundred kilohms, which suggested the connection had been formed between the two microelectrodes. Since the conductivity of CNTs depend on their lattice geometries during their growth process, the conductivities of individual CNTs cannot be well controlled, which results in the variation of conductivities in individual CNTs. During the ac electrophoresis process to form MWNT bundles across microelectrodes, the MWNTs were randomly connected between microelectrodes. Therefore, it is logical that different MWNT samples exhibited different conductivities.

As mentioned in Section II-A, ac electrophoretic manipulation is different from those traditional pick-and-place manipulations (e.g., AFM manipulation), which can only assemble

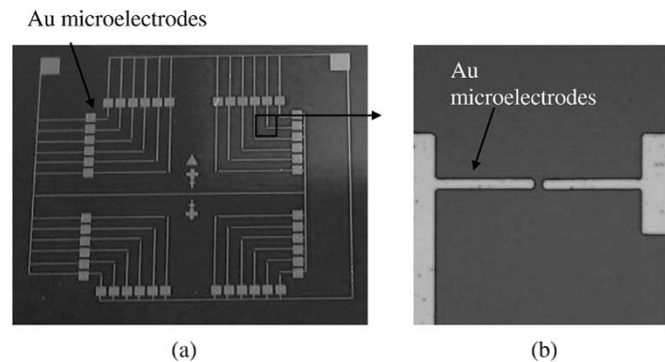


Fig. 9. (a) Photograph of the fabricated array of Au microelectrodes on a substrate. (b) Optical image showing a pair of Au microelectrodes before CNT manipulation.

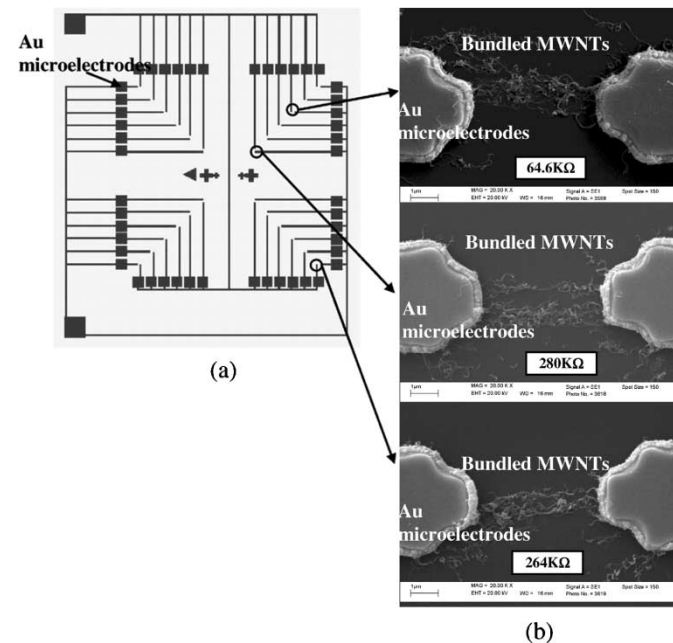


Fig. 10. (a) Drawing of the design for the chip with arrays of Au microelectrodes. (b) SEM images showing the formations of MWNTs between different pairs of Au microelectrodes.

CNT devices one at a time. Instead, ac electrophoretic manipulation is a parallel assembly process where batch assembly of CNT devices is theoretically possible when the electrical potential is applied to an array of microelectrodes that are connected electrically together. To prove the validity of batch assembling by ac electrophoresis, we have implemented the experimental procedures mentioned and extended then to an array of Au microelectrodes that are electrically connected together on a substrate (see Fig. 9). By using the same experimental parameters presented before, we have successfully manipulated the CNT bundles on most of the Au microelectrodes by ac electrophoresis in a single-run fashion. The connections of bundled CNTs for different pairs of microelectrodes on a substrate after addition of one drop of MWNTs/ethanol solution ($\sim 10 \mu\text{L}$) were shown in Fig. 10. In order to confirm the linkage of bundled CNTs across two microelectrodes, the room-temperature resistance corresponding to each pair of microelectrodes was measured. The CNT connection process was deemed successful between two microelectrodes when the room-temperature resistance measured became several to several hundred kilohms.

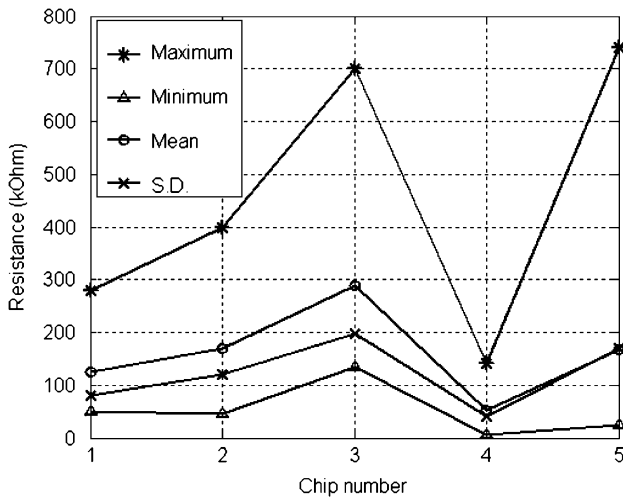


Fig. 11. Plots of statistical data of measured resistances between the Au microelectrodes on different samples.

Several chips were then checked using SEM images to validate the CNT connections between the electrodes.

To validate the consistency of the batch assembly of CNT devices, repeated experiments for ac electrophoretic batch manipulation of CNTs between the arrays of Au microelectrodes were performed and plots of statistical data for different experiments were generated (see Fig. 11), which shows the maximum, minimum, average, and standard deviation (i.e., S.D.) among the measured resistances on each sample. From the experimental results, we have observed that the range of the room-temperature resistances is from several to several hundred kilohms, as stated earlier. Besides, we have experimentally found that the success rate for different sensor chips are consistent with overall success rate, which is equal or greater than 70%. The success rate is defined as the ratio of the number of successful CNT-connected microelectrodes to the total number of microelectrodes on a substrate. Since the volume of each drop of the CNT/ethanol solution in the experiment is not consistent, the yield of the batch assembly of the bundled CNTs cannot be 100% based on our current rudimentary technique. However, the batch ac electrophoretic manipulation of bundled CNTs is efficient and reliable based on our experimental validation, and the yield can be further improved by using a more precise injection system.

III. CNT AS SENSING ELEMENTS FOR THERMAL SENSING

With the ability to batch manipulate the bundled CNTs to form resistive elements on patterned substrates, we have investigated the possibility to utilize the bundled CNTs as sensing elements for thermal sensing. In the following sections, we will present our preliminary electrical characterizations on thermal sensitivity, frequency response, and I - V response of the sensors.

A. Thermal Sensitivity

In order to investigate the temperature dependence of the bundled MWNT sensors, several fabricated sensor chips were packaged on a printed circuit board (PCB) for data acquisition and were put inside an oven (L-C Oven Lab-Line, Instrument Inc., Dubuque, IA). The oven temperature was monitored by a fluke type-K thermocouple at

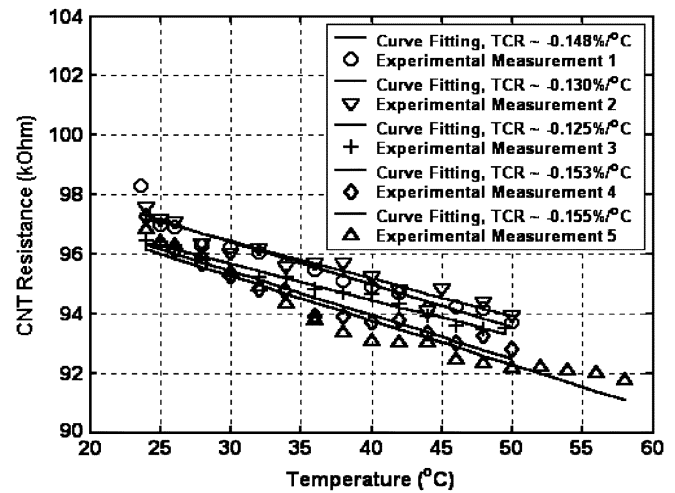


Fig. 12. TCR variations of a typical MWNT device in five consecutive measurements. The experimental data are linearized for the approximation of TCRs.

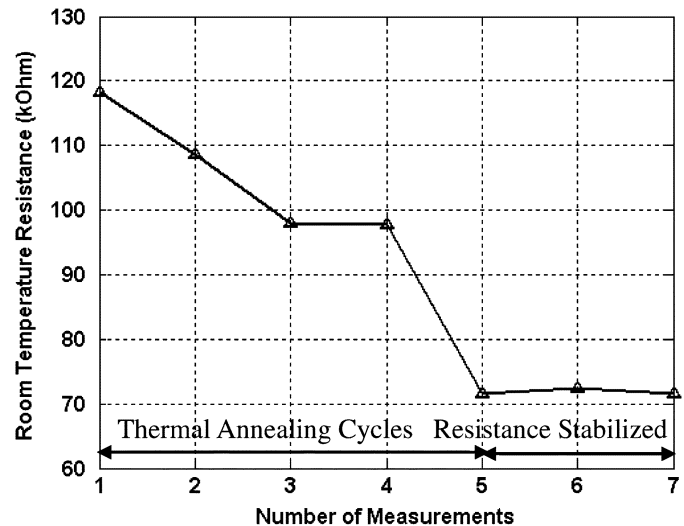


Fig. 13. Room-temperature resistance drifting of the CNT sensors during seven repeated thermal cycling.

tached on the surface of the PCB circuit board. The resistance change of the MWNT sensors were then measured against the temperature inside the oven. The temperature-resistance relationship for the MWNT sensors was measured and a representative data set is shown in Fig. 12 for several cycles of measurements after a few thermal annealing cycles. From the experiments, it was found that a few thermal annealing cycles (from 25 °C to 80 °C for ~ 5 cycles) were necessary before the measured TCRs of the sensor can be stabilized, i.e., considerably room-temperature resistances drift were observed in repeated measurements during the thermal annealing cycles. The statistical data of the room-temperature drift of a typical CNT sensor for each cycle of measurement was measured and plotted in Fig. 13. It was found that the magnitude of the change in resistance during the annealing is $\sim 40\%$ after ~ 5 cycles. The resistance would stabilize afterwards. One possible reason to account for this phenomenon is that during the thermal cycling processes, some CNTs with weak adhesion with the Au microelectrodes may detach from them due to mismatch in the temperature coefficient of expansion, causing

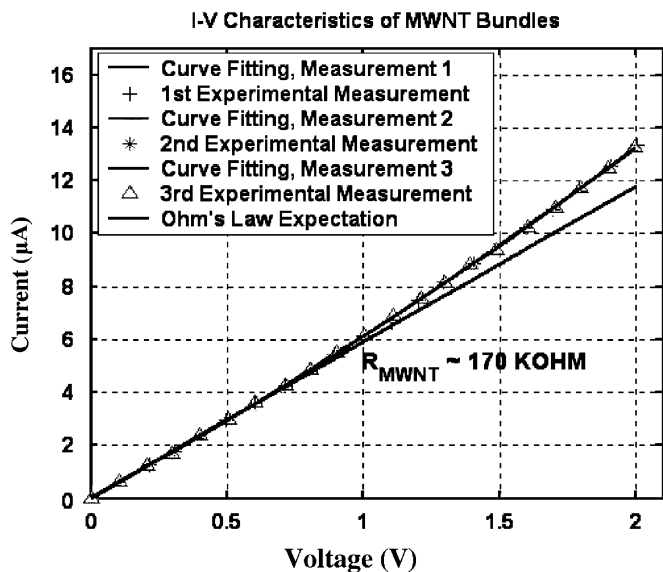


Fig. 14. I - V characteristics of the MWNT bundles. Three repeated measurements were performed to validate the repeatability. The straight line is the theoretical expectation using Ohm's law and the room-temperature resistance of bundled MWNTs in our testing sample was approximately 170 k Ω .

the drift of the room-temperature resistance after each thermal cycling. Therefore, our current work is to use polymer thin films to protect the CNTs and provide a better fixture of CNTs with the microelectrodes.

The TCR of the bundled MWNT sensors was measured to determine their thermal sensitivity. From the experimental results, the bundled MWNTs were sensitive to the change of temperature and their resistance dropped with increasing temperature. The negative TCR of the MWNTs has been reported previously in [26], though the measurements were based on individual MWNTs. The temperature-resistance dependency of bundled MWNTs implied their thermal sensing capability. Based on experimental results, the TCR for an MWNT sensor was obtained by measuring the resistance change of the bundled MWNTs with the corresponding temperature and calculated based on (5) as follows:

$$R(T) = R_0(1 + \alpha(T - T_0)) \quad (5)$$

where R_0 is the resistance at room temperature T_0 , and α is the TCR. The range of the TCR for the MWNT sensors was found to be from -0.1 to $-0.2\%/^{\circ}\text{C}$.

B. Power Consumption

Electrical properties of individual CNTs have been studied by numerous research groups [26], [27] over the past few years. In this study, we have determined the I - V characteristics of the bundled MWNTs after hybridly integrating the bundled MWNTs into a constant current configuration. Similar to those of individual CNTs reported by other researchers, the bundled MWNTs also showed microwatt power characteristics (see Fig. 14), though bundled MWNTs can be regarded as a complex network of individual CNTs. From the results of experiments conducted on the MWNT sensors, the current required to induce self-heating of the MWNT devices was in the microampere range at several volts, which suggests that bundled CNTs could be used as a resistive element for ultra-low-power consumption

devices. Typically, the two-probe room-temperature resistance of the bundled MWNTs ranged from several to several hundred kilohms, as reported previously, and we conjecture that these variations were mainly contributed by the random connections between MWNT bundles during the ac electrophoresis process. However, there are other possible factors, as it is generally recognized that the CNT resistance among many reported experiments varied (e.g., see [28] and [29]). It was reported in [28] that several factors such as quality of the nanotubes and the electrical contacts may account for the variations of the measured resistance across CNTs. The existence of metal-nanotube contact resistance was explained theoretically in [29], i.e., in an idealized model, conduction between the CNT and metal may be forbidden by the Block symmetry of the electrodes. On the other hand, it was studied experimentally that contact resistance in the order of hundreds of kilohms or megaohms was measured when positioning a single CNT on a metal electrode [30] or depositing metal electrodes across a selected signal CNT [31]. Besides, it was indicated in [32] that contact resistance exists between the nanotube bundles and the metal electrodes due to observed discrepancy of three orders of magnitude when different methods were used to measure the resistance. Therefore, the contact resistance should have an influence on the variation of resistance. The magnitude of contact resistance of our sensors has to be further investigated in the future. Nevertheless, several groups have reported that the contact resistance can be decreased by orders of magnitudes by post-treatments such as local electron beam exposure [28], rapid thermal annealing process [33], electroplated Au over the contacted electrodes [34], and focused ion beam to deposit metal on CNT, which showed that the contact resistances were decreased below 100 Ω or in the range of a few tens of ohms [30]. Hence, future work for our group will involve applying one of these techniques to reduce the contact resistance of the CNT sensors.

Despite the random variations in room-temperature resistance of different MWNT bundles, it was found that all of the samples have similar I - V characteristics. In comparison, the operation power of conventional microelectromechanical systems (MEMS) polysilicon sensors is in the order of milliwatts [35]. In other words, the power consumption of CNT-based sensors is three orders of magnitude lower than that of MEMS polysilicon-based sensors.

C. Frequency Response of the Electronic Circuit With a Bundled MWNT as a Feedback Resistor

The frequency response of a sensor measures its efficiency to pick up time-dependent input changes from the surrounding environment. In order to pick up time-dependent fluctuations of the sensing environment, sensors with fast frequency response are highly desired. For turbulent boundary layer research in the field of aerodynamics, shear stress sensors with fine resolution ($<100 \mu\text{m}$), fast frequency response ($>5 \text{ kHz}$) and high sensitivity are highly sought [36].

A typical bundled MWNT sensing element was connected in a constant current mode configuration in the frequency-response experiment (see Fig. 15). To test the frequency response of the driving circuitry with a bundled MWNT as a feedback resistor, an input square wave of 2 V peak-to-peak at 10 kHz was fed into the negative input terminal of the circuit shown in Fig. 15 and

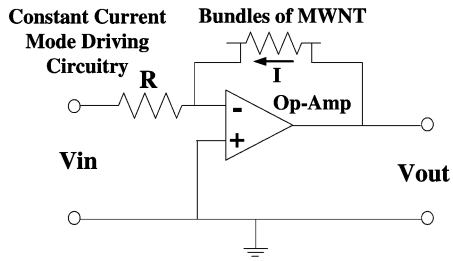


Fig. 15. Schematic diagram showing the constant current mode circuit configuration.

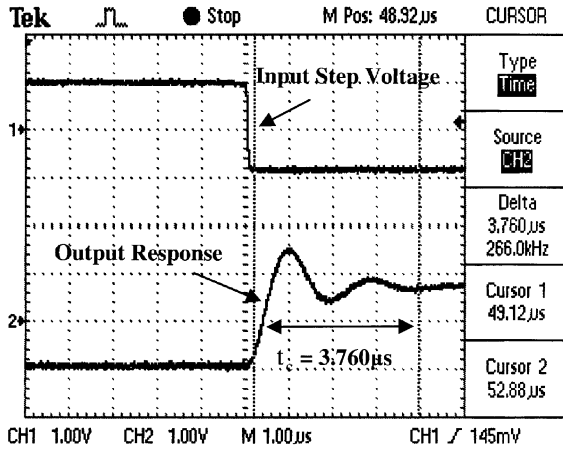


Fig. 16. Frequency response of the constant current circuit with a bundled MWNT as a feedback resistor. The cutoff frequency was estimated to be 177 kHz according to [35].

the output response was determined (see Fig. 16). From our experimental measurements, the electronic circuit with a bundled MWNT as a feedback resistor exhibited very fast frequency response to the input electronic signal. Using the approximation between the time constant and cutoff frequency [35],

$$f_c = 1/1.5t_c \quad (6)$$

where f_c is the cutoff frequency and t_c is the time constant of the response, the estimated cutoff frequency of the system was approximately 177 kHz. As a comparison, a typical frequency response of the constant current mode circuitry with MEMS polysilicon sensors as feedback resistors without frequency compensation is around several hundred hertz to several kilohertz [37].

IV. CONCLUSION

A technique to batch fabricate nanosensors with CNTs based on DEP manipulation has been presented. We have proven that the success rate for batch assembling bundled CNTs on arrays of microelectrodes is equal or greater than 70%, which has demonstrated that DEP manipulation is a feasible technology to batch assemble CNT functional devices. We have also proven that the ac electric field can direct MWNTs to specific areas of a substrate with patterned microelectrodes. With specially designed microelectrodes, bundled MWNTs can be aligned into different directions according to the electric-field generation. The simulation results for the electric-field distribution for different designs of microelectrode geometries has also been presented. With the ability to manipulate the bundled

MWNTs on microfabricated electrodes, bundled MWNTs were investigated as a sensing element for microthermal sensing applications. We have successfully integrated the CNT sensor into a constant current mode configuration for dynamic characterizations such as frequency response, and also for I - V and TCR measurements. Due to the ultra-low-power consumption (in the range of microwatts) and fast frequency response (~ 100 kHz) of the electronic circuit with a bundled MWNT as feedback resistors, CNT-based sensors were shown to be promising in thermal sensing applications.

ACKNOWLEDGMENT

The authors would like to sincerely thank Dr. W. Y. Cheung, Department of Electronic Engineering, CUHK, and K. W. C. Lai and G. M. H. Chan, both of the Centre for Micro and Nano Systems, CUHK, for their help and discussion on this project.

REFERENCES

- [1] S. Iijima, "Helical microtubules of graphitic carbon," *Nature*, vol. 354, pp. 56–58, 1991.
- [2] S. Frank, P. Poncharal, Z. L. Wang, and W. A. de Heer, "Carbon nanotube quantum resistors," *Science*, vol. 280, pp. 1744–1746, 1998.
- [3] E. W. Wong, P. E. Sheehan, and C. M. Lieber, "Nanobeam mechanics: Elasticity, strength, and toughness of nanorods and nanotubes," *Science*, vol. 277, pp. 1971–1975, 1997.
- [4] S. J. Tans, A. R. M. Verschueren, and C. Dekker, "Room-temperature transistor based on a single carbon nanotube," *Nature*, vol. 393, pp. 49–52, 1998.
- [5] T. Rueckes, K. Kim, E. Joselevich, G. Y. Tseng, C. Cheung, and C. M. Lieber, "Carbon nanotube based nonvolatile random access memory for molecular computer," *Science*, vol. 289, pp. 94–97, 2000.
- [6] A. M. Fennimore, T. D. Yuzvinsky, W. Q. Han, M. S. Fuhrer, J. Cumings, and A. Zettl, "Rotational actuators based on carbon nanotubes," *Nature*, vol. 424, pp. 408–410, 2003.
- [7] T. Shiokawa, K. Tsukagoshi, K. Ishibashi, and Y. Aoyagi, "Nanostructure construction in single-walled carbon nanotubes by AFM manipulation," in *Proc. Microprocesses and Nanotechnology Conf.*, 2001, pp. 164–165.
- [8] P. A. Willams, S. J. Papadakis, and M. R. Falvo, "Controlled placement of an individual carbon nanotube onto a microelectromechanical structure," *Appl. Phys. Lett.*, vol. 80, no. 14, pp. 2574–2576, 2002.
- [9] F. Kim, S. Kwan, J. Akana, and P. Yang, "Langmuir–Blodgett nanorod assembly," *J. Amer. Chem. Soc.*, vol. 123, no. 18, pp. 4360–4361, 2001.
- [10] D. Appell, "Wired for success," *Nature*, vol. 419, pp. 553–555, 2002.
- [11] B. Q. Wei, R. Vajtai, Y. Jung, J. Ward, R. Zhang, G. Ramanath, and P. M. Ajayan, "Organized assembly of carbon nanotubes," *Nature*, vol. 416, pp. 495–496, 2002.
- [12] F. C. Cheong, K. Y. Lim, C. H. Sow, J. Lin, and C. K. Ong, "Large area patterned arrays of aligned carbon nanotube via laser trimming," *Nanotechnology*, vol. 14, pp. 433–437, 2003.
- [13] K. Yamamoto, S. Akita, and Y. Nakayama, "Orientation of carbon nanotubes using electrophoresis," *Jpn. J. Appl. Phys.*, vol. 35, pp. L917–L918, 1996.
- [14] —, "Orientation and purification of carbon nanotubes using AC electrophoresis," *J. Phys. D, Appl. Phys.*, vol. 31, pp. L34–L36, 1998.
- [15] P. A. Smith, C. D. Nordquist, T. N. Jackson, T. S. Mayer, B. R. Martin, J. Mbindyo, and T. E. Mallouk, "Electric-field assisted assembly and alignment of metallic nanowires," *Appl. Phys. Lett.*, vol. 77, no. 9, pp. 1399–1401, 2000.
- [16] L. A. Nagahara, I. Amlani, J. Lewenstein, and R. K. Tsui, "Directed placement of suspended carbon nanotubes for nanometer-scale assembly," *Appl. Phys. Lett.*, vol. 80, no. 20, pp. 3826–3828, 2002.
- [17] H. A. Pohl, *Dielectrophoresis: The Behavior of Neutral Matter in Nonuniform Electric Fields*. Cambridge, U.K.: Cambridge Univ. Press, 1978.
- [18] A. Ramos, H. Morgan, N. G. Green, and A. Castellanos, "AC electrokinetics: A review of forces in microelectrode structures," *J. Phys. D, Appl. Phys.*, vol. 31, pp. 2338–2353, 1998.
- [19] T. Heida, W. L. C. Rutten, and E. Marani, "Understanding dielectrophoretic trapping of neuronal cells: Modeling electric field, electrode-liquid interface and fluid flow," *J. Phys. D, Appl. Phys.*, vol. 35, pp. 1592–1602, 2002.

- [20] T. B. Jones, *Electromechanics of Particles*. Cambridge, U.K.: Cambridge Univ. Press, 1995.
- [21] C. A. Grimes, E. C. Dickey, C. Mungle, K. G. Ong, and D. Qian, "Effect of purification of the electrical conductivity and complex permittivity of multiwall carbon nanotubes," *J. Appl. Phys.*, vol. 90, no. 8, pp. 4134–4137, 1995.
- [22] P. Petong, R. Pottel, and U. Kaatz, "Water-ethanol mixtures at different compositions and temperatures. A dielectric relaxation study," *J. Phys. Chem. A*, vol. 104, pp. 7420–7428, 2000.
- [23] X.-B. Wang, Y. Huang, R. Hoize, J. P. H. Burt, and R. Pethig, "Theoretical and experimental investigations of the interdependence of the dielectric, dielectrophoretic and electrorotational behavior of colloidal particles," *J. Phys. D, Appl. Phys.*, vol. 26, pp. 312–322, 1993.
- [24] X. Wang, X.-B. Wang, F. F. Becker, and P. R. C. Gascoyne, "A theoretical method of electrical field analysis for dielectrophoretic electrode arrays using Green's theorem," *J. Phys. D, Appl. Phys.*, vol. 29, pp. 1649–1660, 1996.
- [25] V. T. S. Wong and W. J. Li, "Dependence of AC electrophoresis carbon nanotube manipulation on microelectrode geometry," *Int. J. Nonlinear Sci. Numer. Simulation*, vol. 3, no. 3–4, pp. 769–774, 2002.
- [26] T. W. Ebbesen, H. J. Lezec, H. Hiura, J. W. Bennett, H. F. Ghaemi, and T. Thio, "Electrical conductivity of individual carbon nanotubes," *Nature*, vol. 382, pp. 54–56, 1996.
- [27] P. G. Collins, M. S. Arnold, and P. Avouris, "Engineering carbon nanotubes and nanotube circuits using electrical breakdown," *Science*, vol. 292, pp. 706–709, 2001.
- [28] A. Bachtold, M. Henny, C. Terrier, C. Strunk, and C. Schonenberger, "Contacting carbon nanotubes selectively with low-ohmic contacts for four-probe electric measurements," *Appl. Phys. Lett.*, vol. 73, no. 2, pp. 274–276, 1998.
- [29] J. Tersoff, "Contact resistance of carbon nanotubes," *Appl. Phys. Lett.*, vol. 74, no. 15, pp. 2122–2124, 1999.
- [30] B. Q. Wei, R. Vajtai, and P. M. Ajayan, "Reliability and current carrying capacity of carbon nanotubes," *Appl. Phys. Lett.*, vol. 79, no. 8, pp. 1172–1174, 2001.
- [31] F. Wakaya, K. Katayama, and K. Gamo, "Contact resistance of multiwall carbon nanotubes," *Microelectron. Eng.*, vol. 67–68, pp. 853–857, 2003.
- [32] L. Marty, V. Bouchiat, A. M. Bonnot, M. Chaumont, T. Fournier, S. Decossas, and S. Roche, "Batch processing of nanometer-scale electrical circuitry based on *in-situ* grown single-walled carbon nanotubes," *Microelectron. Eng.*, vol. 61–62, pp. 485–489, 2002.
- [33] J. O. Lee, C. Park, J. J. Kim, J. H. Kim, K. W. Park, and K. H. Yoo, "Formation of low-resistance ohmic contacts between carbon nanotube and metal electrodes by a rapid thermal annealing method," *J. Phys. D, Appl. Phys.*, vol. 33, pp. 1953–1956, 2000.
- [34] D. W. Austin, A. A. Puretzky, D. B. Geohegan, P. F. Britt, M. A. Guillorn, and M. L. Simpson, "The electrodeposition of metal at metal/carbon nanotube junctions," *Chem. Phys. Lett.*, vol. 361, pp. 525–529, 2002.
- [35] C. Liu, J. B. Huang, Z. Zhu, F. Jiang, S. Tung, Y. C. Tai, and C. M. Ho, "A micromachined flow shear-stress sensor based on thermal transfer principle," *J. Microelectromech. Syst.*, vol. 8, pp. 90–99, Mar. 1999.
- [36] J. B. Huang, C. Liu, F. Jiang, S. Tung, Y. C. Tai, and C. M. Ho, "Fluidic shear stress measurement using surface-micromachined sensors," in *Proc. IEEE Region 10 Int. Microelectronics and VLSI Conf.*, 1995, pp. 16–19.
- [37] J. B. Huang, F. K. Jiang, Y. C. Tai, and C. M. Ho, "MEMS-based thermal shear-stress sensor with self-frequency compensation," *Meas. Sci. Technol.*, vol. 10, no. 8, pp. 687–696, 1999.



Carmen K. M. Fung (S'03) received the B.Eng. degree in mechanical and automation engineering and M. Phil. degree in automation and computer-aided engineering from The Chinese University of Hong Kong (CUHK), Shatin, Hong Kong, in 2000 and 2002, respectively, and is currently working toward the Ph.D. degree in automation and computer-aided engineering of The Chinese University of Hong Kong.

Her research interest is the development of technologies for microautomation/nanoautomation and micromanipulation/nanomanipulation, and microsensors/nanosensors.

Ms. Fung was the recipient of the 2000 Best Student Paper Award presented at the 2000 International Conference on Information Society in the 21st Century (IS2000), Aizu, Japan, the 2000 Academic Creativity Award presented by Chung Chi College, CUHK, and the 2003 Best Poster Paper Award presented at the IEEE International Conference on Nanotechnology, San Francisco, CA.



Victor T. S. Wong (S'01) received the B.Eng. degree in automation and computer-aided engineering from The Chinese University of Hong Kong (CUHK), Shatin, Hong Kong, in 2003, and currently working toward the M.Sc. degree at the University of California at Los Angeles (UCLA).

From 2001 to 2003, he was a Student Researcher with the Centre for Micro and Nano Systems, CUHK. He is currently a Graduate Student Researcher with the Institute for Cell Mimetic Space Exploration (CMISE), Los Angeles, CA. His current

research interests include the development of micromanipulation/nanomanipulation technologies, microfabrication/nanofabrication technologies and microsensors/nanosensors and microactuators/nanoactuators.

Mr. Wong was the recipient of the 2001 Lucent Global Science Scholar Award, the 2003 Second Prize Award of the IEEE Region 10 Undergraduate Student Paper Contest, and the 2003 Best Poster Paper Award presented at the IEEE International Conference on Nanotechnology, San Francisco, CA.



Rosa H. M. Chan (S'02) received the B.Eng. degree in automation and computer-aided engineering from The Chinese University of Hong Kong (CUHK), Shatin, Hong Kong, in 2003, and is currently working toward the M.Phil. degree in automation and computer-aided engineering at CUHK.

She had studied computer animation and visual effects at New York University (NYU) in 2001. Her research interest is to develop micromanipulation/nanomanipulation technologies.

Ms. Chan is a student member of the Hong Kong Institution of Engineers (HKIE). Her NYU studies were funded by the Hong Kong Productivity Council and Film Development Fund. In 2002, she joined the University Mobility in Asia and the Pacific (UMAP) Leaders Program and was with the Aerospace Applied Physics Laboratory, Department of Aeronautics and Astronautics, Kyushu University, which was funded by a scholarship from the Association of International Exchange, Japan. She was also the recipient of a 2003 scholarship from the HKIE Manufacturing and Industrial Engineering Division.



Wen J. Li (S'97–A'97–M'00) received the B.S. and M.S. degrees in aerospace engineering from the University of Southern California (USC), Los Angeles, in 1987 and 1989, respectively, and the Ph.D. degree with a specialization in MEMS from the University of California at Los Angeles (UCLA), in 1997.

His industrial experience includes The Aerospace Corporation, El Segundo, CA, Silicon Microstructures Inc., Fremont, CA, and the National Aeronautics and Space Administration (NASA)/California Institute of Technology (Caltech) Jet Propulsion

Laboratory, Pasadena, CA. In 1997, he joined the Department of Automation and Computer-Aided Engineering, The Chinese University of Hong Kong (CUHK), Shatin, Hong Kong. He also serves as the Director of the Centre for Micro and Nano Systems, CUHK. He has authored or coauthored over 130 papers appearing in international journals and conference proceedings on MEMS and nanotechnology related work over the last six and one-half years. His research interest is the development of MEMS devices for micro/nano sensing and manipulation.

Dr. Li is currently the guest editor for the "Focused Section on Micro and Nano Manipulations" of the IEEE/ASME TRANSACTIONS ON MECHATRONICS. He is a member of the Technical Committee on Nanorobotics and Nanomanufacturing of the IEEE Nanotechnology Council. He is also a Distinguished Overseas Scholar of the Chinese Academy of Sciences. He was the recipient of the Aerospace Corporate Fellowship, Silicon Microstructures Inc. Employee Award, and a NASA technical innovation award.